

REPORT DOCUMENTATION PAGE				Form Approved OMB No. 0704-0188	
Public reporting burden for this collection of information is estimated to average 1 hour per response, including the time for reviewing instructions, searching existing data sources, gathering and maintaining the data needed, and completing and reviewing this collection of information. Send comments regarding this burden estimate or any other aspect of this collection of information, including suggestions for reducing this burden to Department of Defense, Washington Headquarters Services, Directorate for Information Operations and Reports (0704-0188), 1215 Jefferson Davis Highway, Suite 1204, Arlington, VA 22202-4302. Respondents should be aware that notwithstanding any other provision of law, no person shall be subject to any penalty for failing to comply with a collection of information if it does not display a currently valid OMB control number. PLEASE DO NOT RETURN YOUR FORM TO THE ABOVE ADDRESS.					
1. REPORT DATE (DD-MM-YYYY) 10-05-2006		REPORT TYPE Journal Article		3. DATES COVERED (From - To) 4 Nov 05 – 10 May 06	
4. TITLE AND SUBTITLE Hydrothermal Growth and Photoluminescence of Zn1-xMgxO Alloy Crystals .				5a. CONTRACT NUMBER IN-HOUSE	
				5b. GRANT NUMBER	
				5c. PROGRAM ELEMENT NUMBER 61102F	
6. AUTHOR(S) Michael Callahan, Lionel Bouthillette and *Buguo Wang				5d. PROJECT NUMBER 2305	
				5e. TASK NUMBER HC	
				5f. WORK UNIT NUMBER 01	
7. PERFORMING ORGANIZATION NAME(S) AND ADDRESS(ES) Optoelectronic Technology Branch, AFRL/RHHC, 80 Scott Drive, Hanscom AFB, MA 01731; * Solid State Scientific Corp., 27-2 Wright Road, Hollis, NH 03049				8. PERFORMING ORGANIZATION REPORT	
9. SPONSORING / MONITORING AGENCY NAME(S) AND ADDRESS(ES) Electromagnetics Technology Division Source Code: 437890 Sensors Directorate Air Force Research Laboratory 80 Scott Drive Hanscom AFB MA 01731-2909				10. SPONSOR/MONITOR'S ACRONYM(S) AFRL-RY-HS	
				11. SPONSOR/MONITOR'S REPORT NUMBER(S) AFRL-RY-HS-TP-2008-0017	
12. DISTRIBUTION / AVAILABILITY STATEMENT DISTRIBUTION A: APPROVED FOR PUBLIC RELEASE: DISTRIBUTION UNLIMITED.					
13. SUPPLEMENTARY NOTES The U. S. Government is joint author of this work and has the right to use, modify, reproduce, release, perform, display, or disclose the work. Published in Crystal Growth & Design, XXXX VOL. 0, NO. 0 1-5, © xxxx American Chemical Society, Published on web on 10 May 2006. Cleared for Public Release by ESC/PA/ESC-06-0499.					
14. ABSTRACT Zn1-xMgxO alloy formation via band gap engineering is important in the development of blue-UV optoelectronic devices by providing lattice-matched transparent substrates for ZnO and nitride-related devices. Zn1-Mgx0 alloy single crystals (Zn0.97MgO.030 and Zn0.945MgO.0550) have been successfully grown by the hydrothermal technique. The growth experiments were carried out at 650 °c and 15-18 kpsi in alkaline solutions. Zn1-xMgxO alloy crystals were formed at pressures below 22 kpsi at the growth temperature of 650 °c. These conditions are similar to the formation of MgO under hydrothermal conditions. A thin ZnO layer formed on the surface of the ZnMgO crystals as the autoclaves cooled to room temperature. After the ZnO layer was removed by etching or polishing from both the Zn0.97MgO.030 and Zn0.945MgO.0550 samples, blue shifts of the photoluminescence emission from the 3.364 eV line of pure ZnO to 3.414 and 3.447 eV, respectively, were measured at ~ 18 K. The composition of the alloys was confirmed by using secondary ion mass spectroscopy (SIMS) elemental analysis. X-ray diffraction indicated that the alloy crystals have good structural quality, whereas the lattice parameters are smaller than those of pure ZnO (for Zn0.945MgO.0550 a) 3.2416 Å, c) 5.1998 Å) because the radius of Mg2+ is smaller than that of Zn2+.					
15. SUBJECT TERMS hydrothermal growth, photoluminescence, crystal growth					
16. SECURITY CLASSIFICATION OF: Unclassified			17. LIMITATION OF ABSTRACT SAR	18. NUMBER OF PAGES 6	19a. NAME OF RESPONSIBLE PERSON Michael Callahan
a. REPORT Unclassified	b. ABSTRACT Unclassified	c. THIS PAGE Unclassified			19b. TELEPHONE NUMBER (include area code) N/A

Hydrothermal Growth and Photoluminescence of $\text{Zn}_{1-x}\text{Mg}_x\text{O}$ Alloy Crystals

Buguo Wang*

Solid State Scientific Corporation, 27-2 Wright Road, Hollis, New Hampshire 03049

M. J. Callahan* and L. O. Bouthillette

Sensors Directorate, Air Force Research Laboratory, Hanscom AFB, Massachusetts 01731

Received August 9, 2005; Revised Manuscript Received April 13, 2006

ABSTRACT: $\text{Zn}_{1-x}\text{Mg}_x\text{O}$ alloy formation via band gap engineering is important in the development of blue–UV optoelectronic devices by providing lattice-matched transparent substrates for ZnO and nitride-related devices. $\text{Zn}_{1-x}\text{Mg}_x\text{O}$ alloy single crystals ($\text{Zn}_{0.97}\text{Mg}_{0.03}\text{O}$ and $\text{Zn}_{0.945}\text{Mg}_{0.055}\text{O}$) have been successfully grown by the hydrothermal technique. The growth experiments were carried out at 650 °C and 15–18 kpsi in alkaline solutions. $\text{Zn}_{1-x}\text{Mg}_x\text{O}$ alloy crystals were formed at pressures below ~22 kpsi at the growth temperature of 650 °C. These conditions are similar to the formation of MgO under hydrothermal conditions. A thin ZnO layer formed on the surface of the ZnMgO crystals as the autoclaves cooled to room temperature. After the ZnO layer was removed by etching or polishing from both the $\text{Zn}_{0.97}\text{Mg}_{0.03}\text{O}$ and $\text{Zn}_{0.945}\text{Mg}_{0.055}\text{O}$ samples, blue shifts of the photoluminescence emission from the 3.364 eV line of pure ZnO to 3.414 and 3.447 eV, respectively, were measured at ~18 K. The composition of the alloys was confirmed by using secondary ion mass spectroscopy (SIMS) elemental analysis. X-ray diffraction indicated that the alloy crystals have good structural quality, whereas the lattice parameters are smaller than those of pure ZnO (for $\text{Zn}_{0.945}\text{Mg}_{0.055}\text{O}$ $a = 3.2416$ Å, $c = 5.1998$ Å) because the radius of Mg^{2+} is smaller than that of Zn^{2+} .

1. Introduction

Research on zinc oxide and its alloys has seen a surge of activity because of their potential for optoelectronic devices.^{1,2} One of the important steps for the design of ZnO-based optoelectronic devices is the realization of band gap engineering by alloying ZnO with other metallic oxides. The ZnMgCdO alloy system has certain advantages over the AlGaInN alloy system, such as higher exciton binding energies, ability to grow direct band gap alloys from green to UV with a smaller change in lattice constants, availability of large lattice-matched substrates, lower growth temperatures, and faster etch rates.

Like many other semiconductor ternary systems, ZnO alloys with various compounds give one the ability to control their energy band gap. ZnMgO is an appropriate candidate as barrier material for ZnO quantum wells; the incorporation of magnesium increases the band gap linearly as a function of Mg concentration in $\text{Zn}_{1-x}\text{Mg}_x\text{O}$ films.³ Narrowing of the band gap can be achieved by the incorporation of cadmium into the ZnO crystal; the band gap decreases monotonically (but not linearly) from 3.3 to 2.9 eV with Cd concentration up to 8%. $\text{Zn}_{1-x}\text{Mg}_x\text{O}$ films and $\text{Zn}_{1-x}\text{Cd}_x\text{O}$ films on sapphire and ZnO–ZnMgO quantum well structures have been grown by pulsed laser deposition (PLD),^{4,5} molecular beam epitaxy (MBE),⁶ and metal organic vapor-phase epitaxy (MOVPE).⁷ It was also reported recently that ZnMgO films can be grown by liquid-phase epitaxy.⁸

ZnO has a wurtzite structure with a band gap of 3.364 eV; MgO has a rock-salt structure with a band gap of 8.4 eV. Intense ultraviolet band edge photoluminescence and excitonic absorption structures were observed at room temperature in $\text{Zn}_{1-x}\text{Mg}_x\text{O}$ films with up to 36 atomic percent Mg incorporation. The band gap varies linearly from 3.3 to 4.2 eV with Mg content. Beyond 36%, phase separation of MgO and ZnO takes place, and when Mg concentration is higher than 62%, $\text{Zn}_{1-x}\text{Mg}_x\text{O}$ films crystallize in the cubic structure with a lattice parameter close to that of MgO.^{3,4}

There are no reports on hydrothermal growth of $\text{Zn}_{1-x}\text{Mg}_x\text{O}$ alloy crystals. If the hydrothermal technique is able to grow $\text{Zn}_{1-x}\text{Mg}_x\text{O}$ alloy crystals, even though this technique will be limited by the low solubility of MgO in wurtzite $\text{Zn}_{1-x}\text{Mg}_x\text{O}$ alloys, there are some advantages over other techniques: (1) alloys with a uniform

composition; (2) large bulk alloy crystals suitable as substrates for ZnO and nitride-based optoelectronic devices, with improved properties compared with pure ZnO substrates; (3) crystals of high quality due to the growth at near equilibrium conditions at lower temperatures. This paper reports the crystal growth of $\text{Zn}_{1-x}\text{Mg}_x\text{O}$ alloy by the hydrothermal technique, and characterization of the grown alloy by secondary ion mass spectroscopy (SIMS), X-ray diffraction (XRD), and photoluminescence.

2. Experiment

Because a temperature greater than 600 °C is required to grow the alloy, two Temp-Pres René 41 nickel-based autoclaves were used for the experiments. One autoclave has a 140 cm³ internal volume with 2.22 cm ID; the other has a 260 cm³ internal volume with 3.3 cm ID. Both autoclaves are capable of 60 kpsi at 600 °C or 40 kpsi at 700 °C and use a Bridgman-type seal. A platinum liner was used in all experiments to isolate the growth environment, which contains a high concentration of hydroxide as mineralization solution and is very corrosive, from the autoclave walls. The platinum liner has OD 16 mm (14 mm ID), volume 16–33 cm³, and 45–60% fill. Water at the same percent fill was used between the liner and the autoclave to counterbalance the pressure. Potassium hydroxide solution (3–5 N) was used as mineralizer, and pure ZnO single crystals grown in previous hydrothermal experiments were used as seeds. Sintered ZnO powder was used as nutrient. Up to 20 wt % of high purity MgO commercial powder (99.999%) was added into the growth solution. Usually 9–20 g of sintered ZnO and 0.5–5 g of MgO pure powder were used in each run. The details of hydrothermal crystal growth, using Pt liners, are described in refs 9–12.

The grown crystals were analyzed by secondary ion mass spectroscopy (SIMS) to determine the amount of magnesium that was incorporated into the crystals. X-ray diffraction was used to identify the phase formation. Low-temperature photoluminescence (PL) was used to evaluate the optical properties. PL measurements were done at 18 K using a Spex ³/₄ meter grating spectrometer equipped with a photomultiplier tube; the excitation source was a 325 nm CW He–Cd laser. The grown alloy crystals were etched using a 50% HCl solution or polished to remove the grown surface of the samples that might have deposited during autoclave cooling. This “internal” material was compared to the “as-grown” surface in photoluminescence measurements.

3. Results and Discussion

3.1. Growth Conditions for Hydrothermal $\text{Zn}_{1-x}\text{Mg}_x\text{O}$ Crystals. It is known that the growth of zinc oxide crystals can be easily realized in a wide temperature range between 150 and 400 °C in

* E-mail addresses: buguo@solidstatescientific.com; Michael.callahan@hanscom.af.mil.

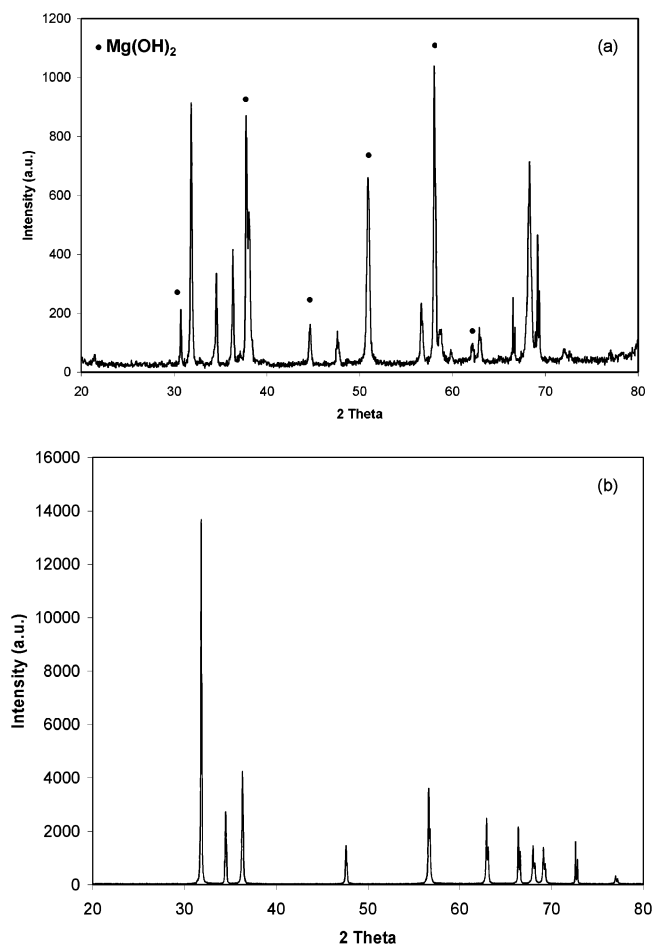
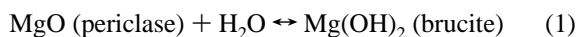


Figure 1. XRD powder diffraction patterns of hydrothermally grown $\text{Zn}_{1-x}\text{Mg}_x\text{O}$:^{19,20} (a) the materials obtained at 350 °C are pure ZnO mixed with $\text{Mg}(\text{OH})_2$; (b) for the crystals obtained at 650 °C, a composition with $\text{Zn}_{0.97}\text{Mg}_{0.03}\text{O}$ was identified. In both cases, the grown single crystals were ground into powder for X-ray powder diffraction.

an autoclave.^{13–15} However, there are no reports on the hydrothermal growth of $\text{Zn}_{1-x}\text{Mg}_x\text{O}$ alloy crystals. Hydrothermal growth of MgO crystals was reported by Webster and White¹⁶ in 1969. Using 12.5 N sodium hydroxide solutions with large temperature gradients ($\Delta T = 150$ °C) along the length of the autoclave, they conducted experiments for growing MgO crystals at 500 bar for 18 h and at growth temperatures from 680 to 790 °C. However, no appreciable growth on the seed crystals was obtained under these conditions. In some experiments, small spontaneously nucleated magnesia crystals formed on the cooler parts of the autoclave liner. Roy et al.¹⁷ reported the phase diagram of $\text{Mg}(\text{OH})_2$ –H₂O in the early 1950s. It was shown that MgO (periclase) phase can be formed only above 700 °C at pressure lower than 1 atm, and $\text{Mg}(\text{OH})_2$ (brucite) is the stable phase at temperatures below 700 °C. Barnes and Ernst¹⁸ reported the phase relations of $\text{Mg}(\text{OH})_2$ –MgO–NaOH in 1963. MgO can be formed from $\text{Mg}(\text{OH})_2$ at 607 °C and 1000 bar or at 634 °C and 1500 bar in the presence of 12.5 M NaOH. MgO and $\text{Mg}(\text{OH})_2$ have an equilibrium as shown by eq 1.



Initially we tried to grow $\text{Zn}_{1-x}\text{Mg}_x\text{O}$ alloy crystals at 350–400 °C in alkaline solutions. No magnesium incorporated into ZnO. Two separate phases^{19,20} of pure ZnO and brucite formed, as shown by X-ray powder diffraction in Figure 1a. To grow $\text{Zn}_{1-x}\text{Mg}_x\text{O}$ alloy crystals by the hydrothermal technique, temperatures higher than those required for pure ZnO crystal growth are necessary. A temperature between 650 and 675 °C was chosen for $\text{Zn}_{1-x}\text{Mg}_x\text{O}$ growth experiments, and nickel-based autoclaves were used to

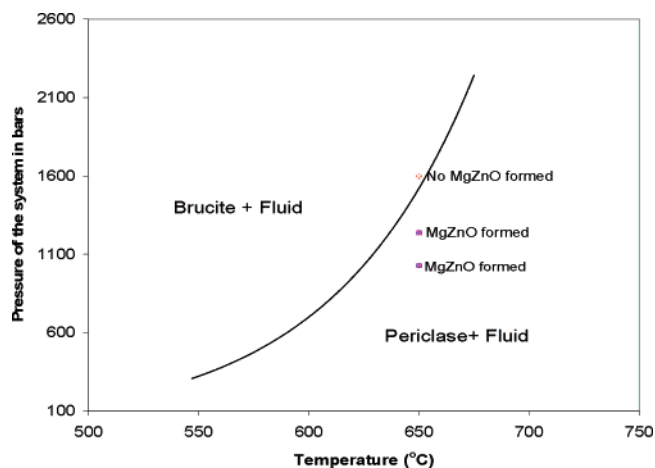


Figure 2. P – T curve for the reaction (brucite = periclase + H₂O) in 12.5 M NaOH solution¹⁸ and the conditions for $\text{Zn}_{1-x}\text{Mg}_x\text{O}$ alloy formation ($x = 0.03$ – 0.055) in 4 N KOH solution (this work).



Figure 3. Photograph of $\text{Zn}_{0.945}\text{Mg}_{0.055}\text{O}$ as grown crystals. Pure ZnO crystals were used as seeds.

accommodate such high temperatures. Successful experiments were carried out when seeds were put in the growth zone at 650 °C and nutrient in the dissolution zone at 660 °C with the pressure at 15–18 kpsi (1025–1237 bar). We found that the ZnO seeds dissolve or no growth occurs if the temperature difference between two zones is smaller than 10 °C.

Pressure is another issue to consider for a successful growth of $\text{Zn}_{1-x}\text{Mg}_x\text{O}$. Since the experiment was run at 650–675 °C, a low pressure is required to avoid autoclave damage, as well as for personnel safety. So a 40–60% fill was used. It was found that in the 650–675 °C temperature range and when the pressure was 24.5 kpsi (1660 bar), no $\text{Zn}_{1-x}\text{Mg}_x\text{O}$ alloy crystals were formed. However, in this same temperature range but with the pressure below 18 kpsi, $\text{Zn}_{1-x}\text{Mg}_x\text{O}$ alloy crystals ($x = 0.03$ – 0.05) did grow. These conditions are similar to formation of MgO under hydrothermal conditions. The pressure–temperature (P – T) conditions of $\text{Zn}_{1-x}\text{Mg}_x\text{O}$ formation in comparison with the data from ref 16 is shown in Figure 2. One can find that the formation conditions of $\text{Zn}_{1-x}\text{Mg}_x\text{O}$ are consistent with the P – T curve obtained from the MgO – $\text{Mg}(\text{OH})_2$ –NaOH system, though the growing crystal is $\text{Zn}_{1-x}\text{Mg}_x\text{O}$ and the mineralizer is KOH. In addition, a condition with a low pressure and a high temperature favors the formation of the $\text{Zn}_{1-x}\text{Mg}_x\text{O}$ phase.

Crystals obtained from two successful hydrothermal growth experiments were characterized as $\text{Zn}_{0.97}\text{Mg}_{0.03}\text{O}$ and

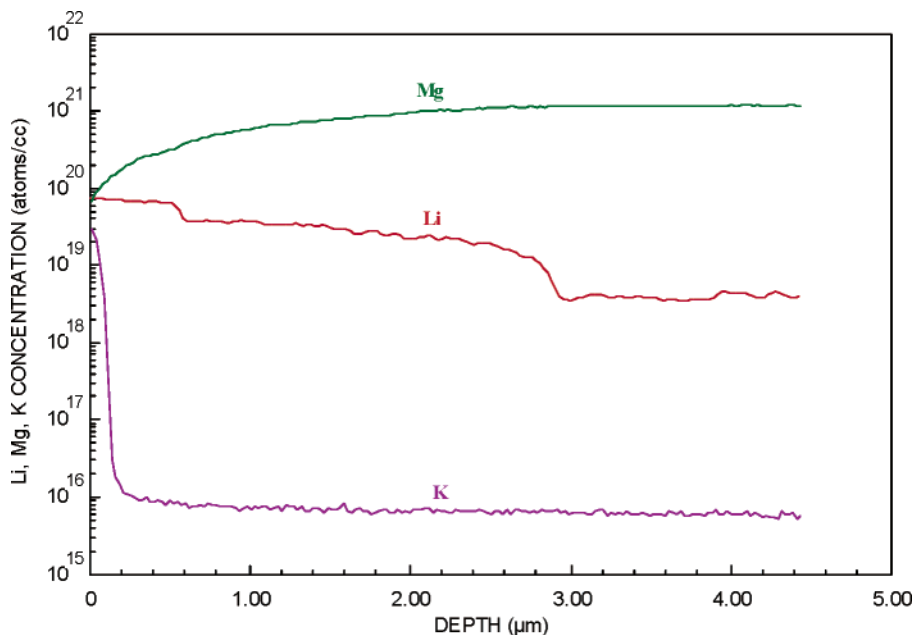


Figure 4. SIMS depth profile of a $\text{Zn}_{0.945}\text{Mg}_{0.055}\text{O}$ crystal.

$\text{Zn}_{0.945}\text{Mg}_{0.055}\text{O}$. Some of the as-grown crystals of $\text{Zn}_{0.945}\text{Mg}_{0.055}\text{O}$ are shown in Figure 3. XRD patterns of these two crystals were the same as that of the pure ZnO, as seen in Figure 1b. However, the lattice parameters of the $\text{Zn}_{0.945}\text{Mg}_{0.055}\text{O}$ crystal calculated from our powder diffraction are $a = 3.2416 \text{ \AA}$, $c = 5.1998 \text{ \AA}$, which is smaller than that of pure ZnO (from JCPDS,¹⁹ $a = 3.2498 \text{ \AA}$, $c = 5.207 \text{ \AA}$) because the radius of the magnesium ion Mg^{2+} (0.057 nm) is smaller than that of Zn^{2+} (0.06 nm).

A SIMS depth profile for the crystal with about 5.5% molar ratio of magnesium incorporation is shown in Figure 4. This analysis shows that the Mg content is about $1.1 \times 10^{21} \text{ atoms/cm}^3$ in this hydrothermally grown $\text{Zn}_{1-x}\text{Mg}_x\text{O}$ alloy. The Mg content in the crystal is also indicated by the band gap blue shift of 83 meV from 3.364 eV of pure ZnO by the PL measurements (see Figure 6). From SIMS results, one can also find that although we used a high concentration of KOH as mineralizer for the experiments, just a small amount of potassium was incorporated in the alloy but a higher concentration of lithium was incorporated due to its small ionic radius.

Because the ionic radii of Mg^{2+} and Zn^{2+} are sufficiently close, a large lattice deformation in the MgZnO structure can be avoided when a low Mg concentration is incorporated in wurtzite structure or a low Zn concentration is incorporated in the cubic structure of MgO . Regarding the low Mg concentration domain in wurtzite MgZnO , the reported thermodynamic solubility limit²⁴ of MgO in ZnO for hexagonal $\text{Zn}_{1-x}\text{Mg}_x\text{O}$ is $x \approx 0.06$. The magnesium concentration in our hydrothermal $\text{Zn}_{0.945}\text{Mg}_{0.055}\text{O}$ alloy is very close to this highest concentration that can be incorporated in ZnO with wurtzite structure by solution growth. However, there are no detailed reports on the highest concentration of MgO can be alloyed with ZnO while the formed alloys are still in the wurtzite structure.^{24–26} Hexagonal epitaxial $\text{Zn}_{1-x}\text{Mg}_x\text{O}$ films with x values up to 36% were reported^{3,26} and were considered as a metastable phase.

If the phase diagram of MgO –ZnO in ref 25 is true, it is unlikely that wurtzite $\text{Zn}_{1-x}\text{Mg}_x\text{O}$ with $0.62 > x > 0.06$ could be grown by the hydrothermal technique. However, cubic $\text{Zn}_{1-x}\text{Mg}_x\text{O}$ ($x > 0.62$) could be grown by the hydrothermal technique if the growth temperature is high and the concentration of MgO – $\text{Mg}(\text{OH})_2$ is greater than that of ZnO – $\text{Zn}(\text{OH})_2$ in the system.

3.2. Photoluminescence Measurements. PL measurements were performed on the samples at room temperature and at $\sim 18 \text{ K}$. Samples were measured as-grown and after removing the surface by polishing or etching. It is important to examine the PL from the

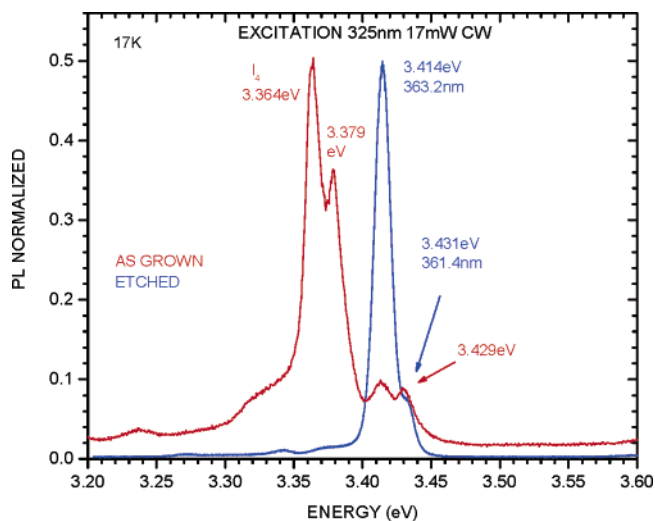


Figure 5. Photoluminescence spectra of as-grown and etched $\text{Zn}_{0.97}\text{Mg}_{0.03}\text{O}$ crystal obtained at 17 K.

“interior” of the alloy because during cooling of the autoclave a thin ZnO layer grows on the surface of the crystal. As shown in Figure 5, the PL spectra of the as-grown $\text{Zn}_{0.97}\text{Mg}_{0.03}\text{O}$ contains near-band-edge emission peaks of both $\text{Zn}_{0.97}\text{Mg}_{0.03}\text{O}$ at 3.414 eV and pure ZnO at 3.364 eV; the peak of pure ZnO at 3.364 eV is much stronger than the peak at 3.414 eV. This means that the as grown material contains a high amount of ZnO on the surface of the alloy crystal. After the as-grown crystal was etched in a HCl solution (about 25% of the weight was etched away), the PL spectra of the etched crystal show no ZnO emission peaks, but the emission peak of $\text{Zn}_{0.97}\text{Mg}_{0.03}\text{O}$ at 3.414 eV becomes stronger. The 50 meV band gap shift after etching indicates that a true alloy was formed and a thin layer of crystalline ZnO on the surface of the alloy was removed. Crystals from another hydrothermal growth experiment were also examined by PL. This as-grown alloy also had multiple emission peaks located at 3.447 and 3.364 eV. Instead of etching, the sample was polished to remove the thin ZnO surface layer that grew during cooling. The PL spectrum after polishing is shown in Figure 6. A strong near-band-edge emission is located at 3.447 eV, about 83 meV higher than pure ZnO near-band-edge emission. From SIMS analysis in Figure 4, this sample contains about 5.5% Mg.

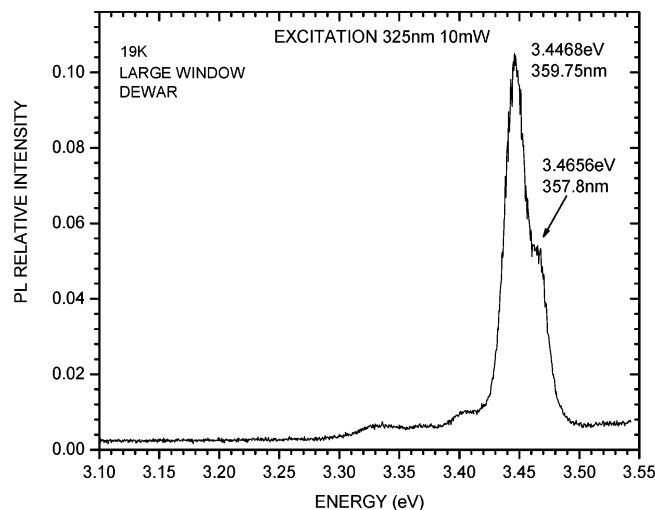


Figure 6. Photoluminescence spectra of $\text{Zn}_{0.945}\text{Mg}_{0.055}\text{O}$ crystal obtained at 19 K. The as-grown crystal was polished instead of etched; about 0.25 mm of the as-grown surface was removed from a 2 mm thick crystal before PL and SIMS measurements.



Figure 7. Schematic drawing of hydrothermally grown $\text{Zn}_{1-x}\text{Mg}_x\text{O}$. The surface is covered by a thin crystalline ZnO layer.

According to ref 3, when $x = 0.33$, the PL of band gap emission of $\text{Zn}_{1-x}\text{Mg}_x\text{O}$ is at 3.87 eV (for pure ZnO, $x = 0$, the PL of band gap emission is at 3.36 eV). Using this result and assuming the bowing parameter is zero, we calculate that the Mg contents in our two alloy crystals are 5.37% and 3.24% respectively. Both compositions are very close to the SIMS analysis for our respective samples. This result is interesting because the $\text{Zn}_{1-x}\text{Mg}_x\text{O}$ in ref 3 was metastable (deposited by PLD) and certainly contained a lot of strains due to deposit on sapphire, whereas our $\text{Zn}_{1-x}\text{Mg}_x\text{O}$ crystals were grown on a nearly homo-epitaxial substrate under nearly equilibrium conditions.

The etching or polishing to remove the ZnO surface layer on the $\text{Zn}_{1-x}\text{Mg}_x\text{O}$ is important. Zinc oxide in 4 M KOH solution at 500–600 °C has a very high solubility (solubility of ZnO in 6 M KOH at 650 °C is about 6 wt %, 4 wt % at 350 °C²¹). When an autoclave is cooled, the solution becomes supersaturated, and ZnO nucleates on the ZnMgO surface without incorporating Mg into the lattice, as shown schematically in Figure 7. According to Hüttig and Müldner²² and Laudise et al.,²³ the temperature for the $\text{Zn}(\text{OH})_2$ –ZnO transition should nearly coincide with the $(\text{H}_2\text{O})_g$ – $(\text{H}_2\text{O})_l$ equilibrium line, and the pressure of water over $\text{Zn}(\text{OH})_2$ –ZnO should nearly equal the vapor pressure of pure

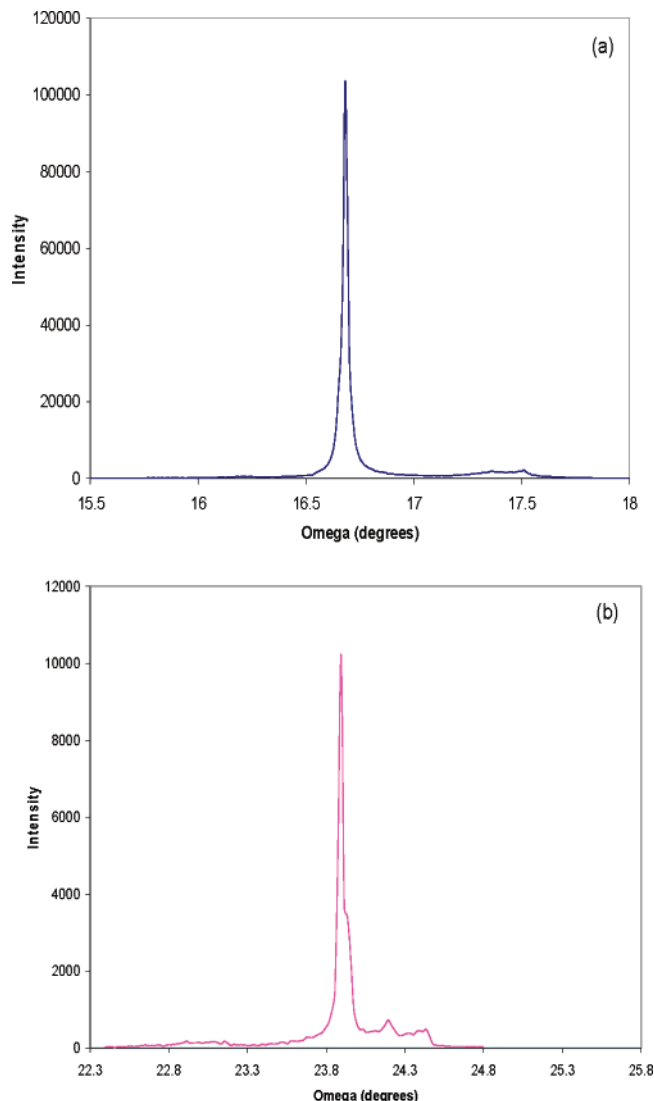


Figure 8. X-ray rocking curves of a hydrothermally grown $\text{Zn}_{0.945}\text{Mg}_{0.055}\text{O}$ measured from the zinc terminated face (double axis ω – 2θ scans): (a) (0 0 0 2) reflection; (b) (1 0 –1 2) reflection. The as-grown surface was ground away before measurement.

water. ZnO is easily formed from $\text{Zn}(\text{OH})_2$ – H_2O even at 50 °C and 1 atm, whereas MgO cannot be formed from $\text{Mg}(\text{OH})_2$ – H_2O when the temperature is lower than 700 °C at 1 atm. When the experiment is interrupted, the growth of $\text{Zn}_{1-x}\text{Mg}_x\text{O}$ crystals stops, but ZnO continues to grow because the solution still is supersaturated due to the temperature decreasing. At the same time, $\text{Mg}(\text{OH})_2$ has different structure and crystallizes separately in the cold zone during cooling.

3.3. High-Resolution X-ray Diffraction. High-resolution X-ray diffraction was also performed on the hydrothermally grown $\text{Zn}_{1-x}\text{Mg}_x\text{O}$ alloy crystals. The ZnO layer coating on the surface was first ground off to reveal the alloy surface. Full width at half-maximum (FWHM) of the rocking curves measured on the zinc face was 100 arcsec for (0 0 0 2) reflection and 150 arcsec for (1 0 –1 2) reflection, as seen in Figure 8. The rocking curves measured on the oxygen face had multiple peaks for (0 0 0 2) reflection; FWHM of (1 0 –1 2) reflection was 500 arcsec. The small line width broadening may be attributed to misfit stress created by the difference between the ZnO seed and the alloy growth. The small peaks in the X-ray diffraction may be due to surface damage from grinding. Nevertheless, the results show that the alloy crystals have good structural quality. Since ZnO seeds were used for the growth of these unmatched alloy crystals, a better result can be expected if perfect alloy seeds were used and the surface was well polished.

4. Conclusion

$\text{Zn}_{1-x}\text{Mg}_x\text{O}$ alloy single crystals up to $10 \times 10 \times 2 \text{ mm}^3$ of uniform composition with $x = 0.03\text{--}0.055$ have been successfully grown by the hydrothermal technique. The growth experiments were carried out at 650°C and $15\text{--}18 \text{ kpsi}$. $\text{Zn}_{0.97}\text{Mg}_{0.03}\text{O}$ and $\text{Zn}_{0.945}\text{Mg}_{0.055}\text{O}$ alloy crystals were obtained. PL spectra of the alloy crystals show blue shifts of the band gap from 3.364 eV ($x = 0$, i.e., pure ZnO) to 3.414 eV ($x = 0.03$) and 3.447 eV ($x = 0.055$). X-ray diffraction indicated that the alloy crystals have good structural quality with lattice parameters smaller than those of pure ZnO due to substitution of Zn^{2+} with smaller Mg^{2+} . The lattice parameters of $\text{Zn}_{0.945}\text{Mg}_{0.055}\text{O}$ crystal calculated from our powder diffraction are $a = 3.2416 \text{ \AA}$, $c = 5.1998 \text{ \AA}$ (for pure ZnO, $a = 3.2498 \text{ \AA}$, $c = 5.207 \text{ \AA}$ ¹⁹). The alloy crystals were coated by a thin layer of crystalline ZnO during cooling of the autoclave. These initial results show the value of using the hydrothermal technique for growing ZnMgO alloys and other ZnO-based alloys to produce lattice-matched transparent substrates with compositional uniformity for ZnO and nitride-related devices. Studies of the formation of $\text{Zn}_{1-x}\text{Mg}_x\text{O}$ and other ZnO alloys through band gap engineering will promote development of ZnO-based optoelectronic devices.

Acknowledgment. This work was conducted at US Air Force Research Laboratory, Hanscom AFB, MA. SIMS elemental analysis was performed by Evans East Inc., NJ. This work was in part funded by the Air Force Office of Scientific Research (Dr. Donald Silversmith, program manager). The authors are indebted to Mr. Michael Suscavage, Dr. David Bliss, and Dr. Michael Alexander for reading the manuscript. Sheng-Qi Wang is acknowledged for performing high-resolution X-ray diffraction on the crystals.

References

- (1) Pearton, S. J.; Norton, D. P.; Ip, K.; Heo, Y. W.; Steiner, T. *Prog. Mater. Sci.* **2005**, *50*, 293–340.
- (2) Triboulet, R.; Perrière, J. *Prog. Cryst. Growth Mater. Charact.* **2003**, *47*, 65–138.
- (3) Ohtomo, A.; Kawasaki, M.; Koida, T.; Masubuchi, K.; Koinuma, H.; Yasuda, T.; Segawa, Y. *Appl. Phys. Lett.* **1998**, *72*, 2466–2468.
- (4) Yang, W.; Hullavarad, S. S.; Nagaraj, B.; Takeuchi, I.; Sharma, R. P.; Venkatesan, T.; Vispute, R. D.; Shen, H. *Appl. Phys. Lett.* **2003**, *82*, 3424–3426.
- (5) Teng, C. W.; Muth, J. F.; Özgür, Ü.; Bergmann, M. J.; Everitt, H. O.; Sharma, A. K.; Jin, C.; Narayan, J. *Appl. Phys. Lett.* **2000**, *76*, 979.
- (6) Sakurai, K.; Kubo, T.; Kajita, D.; Tanabe, T.; Takasu, H.; Fujita, S. *Jpn. J. Appl. Phys.* **2000**, *39*, L1146.
- (7) Gruber, Th.; Kirchner, C.; Kling, R.; Reuss, F.; Waag, A. *Appl. Phys. Lett.* **2004**, *84*, 5359.
- (8) Sato, H.; Ehrentaut, D.; Fukuda, T. *Abstract Book*, 16th American Conference on Crystal Growth and Epitaxy, Big Sky, Montana, 2005, page 105.
- (9) Suscavage, M.; Harris, M.; Bliss, D.; Yip, P.; Wang, S.-Q.; Schwall, D.; Bouthillette, L.; Bailey, J.; Callahan, M.; Look, D. C.; Reynolds, D. C.; Jones, R. L.; Litton, C. W. *MRS Internet J. Nitride Semicond. Res.* **1999**, *4S1*, G3.40.
- (10) Monchamp, R. R.; Puttbach, R. C.; Nielson, J. W. *Hydrothermal growth of zinc oxide crystals*; Technical report AFML-TR-67-144; Airtion Division of Litton Industries: Morris Plains, New Jersey, Contract No. AF33(657)-8795, November, 1964.
- (11) Larkin, J.; Harris, M.; Cornier, J. E.; Armington, A. J. *Cryst. Growth* **1993**, *128*, 871–875.
- (12) Halliburton, L. E.; Wang, L.; Bai, L.; Garces, N. Y.; Giles, N. C.; Callahan, M. J.; Wang, B. J. *Appl. Phys.* **2004**, *96*, 7168.
- (13) Laudise, R. A.; Kolb, E. D.; Caporaso, A. J. *J. Am. Ceram. Soc.* **1964**, *47*, 9–12.
- (14) Croxall, D. F.; Ward, R. C. C.; Wallace, C. A.; Kell, R. C. J. *Cryst. Growth* **1974**, *22*, 117.
- (15) Maeda, K.; Sato, M.; Niikura, I.; Fukuda, T. *Semicond. Sci. Technol.* **2005**, *20*, S49.
- (16) Webster, F. W.; White, E. A. D. *J. Cryst. Growth* **1969**, *5*, 167.
- (17) Roy, D. M.; Roy, R. *Am. J. Sci.* **1957**, *255*, 573.
- (18) Barnes, H. L.; Ernst, W. G. *Am. J. Sci.* **1963**, *261*, 129.
- (19) JCPDS: 36-1451, 21-1486 ZnO XRD data.
- (20) JCPDS: 7-239 for $\text{Mg}(\text{OH})_2$ and 4-0829 for cubic MgO XRD data.
- (21) Laudise, R. A.; Kolb, E. D. *Am. Mineral.* **1963**, *48*, 642.
- (22) Hüttig, G. F.; Müldner, H. Z. *Anorg. Chem.* **1933**, *211*, 368.
- (23) Laudise, R. A.; Ballman, A. A. *J. Phys. Chem.* **1960**, *64*, 688.
- (24) Sarver, J. F.; Katnack, F. L.; Hummel, F. A. *J. Electrochem. Soc.* **1959**, *106*, 960.
- (25) Segnit, E. R.; Holland, A. E. *J. Am. Ceram. Soc.* **1965**, *48*, 409.
- (26) Sharma, A. K.; Narayan, J.; Muth, J. F.; Teng, C. W.; Jin, C.; Kvit, A.; Kolbas, R. M.; Holland, O. W. *Appl. Phys. Lett.* **1999**, *75*, 3327.

CG0504004